

MICROCOPY RESOLUTION TEST CHART
NATIONAL BUREAU OF STANDARDS-1963-A

12

REPORT NO. NADC-83112-30



**VALIDATION OF COMPUTER PROGRAM
CABUOY FOR VERTICAL OSCILLATION OF
SONOBUOY SUSPENSIONS**

AD-A134908

Roger A. Holler
Sensors and Avionics Technology Directorate (Code 3043)
NAVAL AIR DEVELOPMENT CENTER
Warminster, PA 18974

3 OCTOBER 1983

PHASE REPORT
AIRTASK NO. A03S034A/001B/3F11-100-000
Work Unit No. ZU701

Approved for Public Release; Distribution Unlimited

Prepared For
NAVAL AIR SYSTEMS COMMAND
Department of the Navy
Washington, DC 20381

DTIC
EXTRACTED
NOV 23 1983
D
E

DTIC FILE COPY

83 11 23 016

NOTICES

REPORT NUMBERING SYSTEM – The numbering of technical project reports issued by the Naval Air Development Center is arranged for specific identification purposes. Each number consists of the Center acronym, the calendar year in which the number was assigned, the sequence number of the report within the specific calendar year, and the official 2-digit correspondence code of the Command Office or the Functional Directorate responsible for the report. For example: Report No. NADC-78015-20 indicates the fifteenth Center report for the year 1978, and prepared by the Systems Directorate. The numerical codes are as follows:

CODE	OFFICE OR DIRECTORATE
00	Commander, Naval Air Development Center
01	Technical Director, Naval Air Development Center
02	Comptroller
10	Directorate Command Projects
20	Systems Directorate
30	Sensors & Avionics Technology Directorate
40	Communication & Navigation Technology Directorate
50	Software Computer Directorate
60	Aircraft & Crew Systems Technology Directorate
70	Planning Assessment Resources
80	Engineering Support Group

PRODUCT ENDORSEMENT – The discussion or instructions concerning commercial products herein do not constitute an endorsement by the Government nor do they convey or imply the license or right to use such products.

APPROVED BY: Edward J. Jannuzzi DATE: 20 Oct 1983

TABLE OF CONTENTS

	Page
LIST OF FIGURES	i
LIST OF TABLES	ii
SUMMARY	1
INTRODUCTION	1
BACKGROUND	1
RESULTS	1
CONCLUSIONS	2
RECOMMENDATIONS	2
DISCUSSION	3
CABUOY SYSTEM MODEL	3
VERTICAL MOTION VALIDATION MODEL	5
SINGLE DISK SYSTEM	5
SPRING CHARACTERISTICS	6
AMPLITUDE VARIATION	10
TWO DISK SYSTEM	10
CYLINDER SYSTEM	10
ACKNOWLEDGEMENT	11
REFERENCES	12

LIST OF FIGURES

Figure	Title	Page
1	CABUOY (Model Definition)	17
2	Linearization Of Bungee Stress-Strain Curve	18
3	Hydrodynamic Inertia Coefficient Versus Acceleration Modulus For Oscillating Disks ($C_I = m_H/\rho d^3$)	19
4	Drag Coefficient Versus Acceleration Modulus For Oscillating Disks	19
5	Vertical Motion Experimental Arrangement In The 100-Foot NAVSURFWPCEN Undersea Weapons Tank	20
6	Three Body Types Used In The NAVSURFWPCEN 100-Foot Tank Experiment	21
7	Elongation Of The Multistrand Bungee Under Static Tension	22
8	Static And Dynamic Spring Constants For Multistrand Bungee Under Load	23

NADC-83112-30

LIST OF FIGURES (Continued)

Figure	Title	Page
9	Comparison Of Dynamic And Static Equations To Characterize The Multistrand Bungee	24
10	Comparison Of CABUOY Results With Observed Measurements For The Disk System (30-Foot Compliance, 6-Foot p-p Input Amplitude)	25
11	Comparison Of Observed And CABUOY Results For The Disk System (30-Foot Compliance) With 3-Foot And 6-Foot p-p Input Amplitudes	26
12	Comparison Of Calculated Data On Disk System And Observed Data As A Function Of Observed Amplitude	27
13	Comparison Of Single Disk And Two Disk Systems With 3-Foot p-p Input Amplitude (30-Foot Bungee)	28
14	Drag Coefficient Versus Length-To-Diameter Ratio For Oscillating Cylinders	29
15	Hydrodynamic Inertia Coefficient Versus Length-To-Diameter Ratio For Oscillating Cylinders	30
16	Comparison Of Cylinder ($\lambda/d = 0.75$) Oscillation On 30-Foot Bungee With 3 And 6-Foot p-p Input Amplitudes	31
17	Hydrodynamic Mass Coefficient For Low-Aspect Ratio Cylinders For The CABUOY Program (Preliminary)	32

LIST OF TABLES

Table	Title	Page
I	Experimental Data For 12-Inch Diameter Disk On 30-Foot Length of Bungee. (Runs 6-12 For Plexiglas (Rigid) Disk, Runs 13-19 For Plastic (Flexible) Disk With 6-Foot Input Amplitude.)	13
II	Comparison Of CABUOY Calculated Output Using Static And Dynamic Spring Equations With Observed Amplitude Measurements For The Disk System (6-Foot Input Amplitude)	14
III	Experimental Data For 12-Inch Diameter Disk On 30-Foot Bungee With 3-Foot Input Amplitude	14
IV	Comparison Of CABUOY Calculated Output (Using Dynamic Spring Equation) With Observed Measurements For Disk System (3-Foot Input Amplitude)	15

LIST OF TABLES (Continued)

Table	Title	Page
V	Comparison Of CABUOY Calculated Output With Observed Measurements For A Two-Disk System	15
VI	Comparison Of Observed And CABUOY Calculated Motion Of A Cylindrical Weight (L/D = 0.75) On The 30-Foot Length Of Bungee	16

Accession For		
NTIS GRA&I	<input checked="" type="checkbox"/>	
DTIC TAB	<input type="checkbox"/>	
Unannounced	<input type="checkbox"/>	
Justification		
By _____		
Distribution/		
Availability Codes		
Class and/or		
Dist. Statement		
A-1		



SUMMARY

INTRODUCTION

The development and performance evaluation of ASW sonobuoys requires analysis of the sonobuoy interaction with the ocean environment. Ocean currents and waves affect the sensor depth, orientation, self-noise, and survivability and must be taken into account in the earliest phases of sonobuoy design and development. An accurate computer simulation permits early analysis of proposed systems, provides a basis for evaluating changes in the system as the design evolves, and establishes a tool for analyzing performance of component and prototype hardware during test and evaluation.

Perhaps the most useful computer program developed for analysis of sonobuoy systems is entitled CABUOY. This program has the capability of modelling a free-floating, moored, or towed system in a two dimensional ocean current with wave excitations from sinusoids to random sea states. The complexity of a computer program like CABUOY requires an extensive validation to be undertaken. It is only by performing experiments and comparing the computer results with an empirical "ground truth" that confidence in the accuracy of the computer program can be obtained. To this end, a set of validation experiments were conducted to verify computer results.

This report presents the results of the first experimental validation of the CABUOY computer program in the simplest case considered, i.e., the vertical motion of a body suspended in still water at the lower end of an elastic cable when the upper end of the cable (the surface float end) was subjected to vertical harmonic motion.

BACKGROUND

The dynamic representation in a computer program for an ocean deployed system consisting of a surface buoy, connecting cables, and one or more submerged body has been considerable interest to the oceanographic, sonobuoy, and sonar communities. A time domain computer program entitled CABUOY was developed for the Naval Air Development Center (NAVAIRDEVGEN) by the David W. Taylor Naval Ship Research and Development Center (DTNSRDC) to model this ocean deployed buoy system^{1,2,3}.

Because of CABUOY's utility, immediate use was made of the program to model sonobuoy systems. As a result, several modifications were implemented by the NAVAIRDEVGEN and the DTNSRDC to expand or improve the program^{4,5,6,7}.

RESULTS

The validation of the CABUOY program for the vertical motion of a spring-body suspension system in water was successful but only after some revision was made to the program to correct an iteration calculation of virtual mass.

The internal calculations of the (revised) CABUOY program for virtual mass and drag of disks were required for valid results of systems with disks. A single disk and two independent disks in the same suspension were successfully modelled by CABUOY using the internal routine for virtual mass.

The CABUOY modelling of a system with a low-aspect ratio cylinder (and no disk) was only approximate because of the approximation of virtual mass and drag for this body.

CONCLUSIONS

The accuracy of the CABUOY program results depends upon correct user input to characterize the spring, especially a non-linear spring normally used in a sonobuoy system, where attention must be paid to the dynamic as well as static spring properties.

Further data on virtual mass of oscillating bodies is required to permit the user a wider scope of CABUOY validity.

RECOMMENDATIONS

The body of data on the virtual mass and drag of oscillating bodies of various geometries needs to be expanded for across-the-board utilization of the CABUOY program.

A modification to the CABUOY program to permit a more direct input of spring characteristics should be made. This modification might employ a separate static and dynamic spring constant.

A revised program listing and additional user's information should be provided to all those users who have the CABUOY program.

Other aspects of CABUOY should be validated.

DISCUSSION

CABUOY SYSTEM MODEL

CABUOY solves for the dynamic motions of drifting (free floating), moored, or towed systems consisting of a surface float and any combination of suspended bodies and interconnecting cables as shown in figure 1. The surface float can be input as a spheroid, ranging from a thin disk (extreme oblate spheroid) to a spar (extreme prolate spheroid), which interacts with the surface waves, or the float can be directly coupled to or completely decoupled from the surface for prescribed motions under experimental conditions. The cable is divided into a number of rigid (straight line) extensible segments. A body represented by a point mass of known drag area and virtual mass may be included between each cable segment, if desired.

The ocean environment includes a user-defined sea surface which decays exponentially with depth. This is generated by the summation of up to nineteen sine waves with various amplitudes, frequencies, and phases. The program will also internally generate sea states⁵. A two dimensional current profile of coplanar horizontal current velocity with water depth is input, as well. The steady-state calculations for the catenary in the current profile use the finite element analysis techniques and iteration routines used in the steady-state free floating and moored system computer programs FF2E and MR3E8, 9.

The cable stress-strain relationship is defined by:

$$T = T_{ref} + C_1 \epsilon^{C_2} + C_{INT} \dot{\epsilon} \quad \text{eq (1)}$$

where

T = cable tension

T_{ref} = constant "reference" tension

C_1, C_2 = constants

C_{INT} = internal damping coefficient

ϵ = strain, i.e., change in length/original length

$\dot{\epsilon}$ = rate of change of strain, $d\epsilon/dt$

For most applications C_{INT} is small and the last term in equation (1) can be neglected. If the cable is a linear spring, $C_2 = 1$ and $C_1 = AE$, where A is the cable cross sectional area and E is the elastic modulus. A linear approximation of the cable is generally made around the operating tension, as illustrated in figure 2. T_{ref} can be found from the T -axis intercept of the linearized curve and $C_1 = dT/d\epsilon$, or the slope of the linear portion of the curve. The computer program uses this equation to determine the static elongation of the cable to relate the dynamic change of tension to the amplitude of the motion of the body (or bodies) attached to the cable(s).

NADC-83112-30

The hydrodynamic effects on a body being moved through a fluid are two-fold. A drag force which resists the motion is velocity dependent as described by the equation:

$$F_D = \frac{\rho}{2} C_D S V^2 \quad \text{eq (2)}$$

where

F_D = drag force

ρ = fluid density

C_D = drag coefficient

S = cross-sectional area of body

V = velocity of the body relative to the fluid

If the body is moving at constant velocity, the drag force (assuming no lift force applies) is the only hydrodynamic effect of concern. However, if the body is accelerated through the fluid, a second effect is of importance, i.e., the hydrodynamic mass. An accelerating body has an effective mass, called the virtual mass, which is defined as

$$m_v = m_p = m_h \quad \text{eq (3)}$$

where

m_v = virtual mass

m_p = physical mass = weight (in air)/gravitational acceleration

m_h = hydrodynamic (or added) mass.

The hydrodynamic mass is more elusive in character than drag because it is more difficult to measure, but it becomes a significant factor in determining the motion of a body oscillating in a fluid. Included as an option in the CABUOY program is an internal calculation of the hydrodynamic mass for disks. Based on a previous empirical investigation¹⁰, this calculation was an iterative operation, determining the hydrodynamic mass and drag of a disk in harmonic acceleration from the peak values of velocity and acceleration according to the following equations:

$$m_h = 1.2 \rho d^3 (V^2/ad)^{1/2} \quad \text{eq (4)}$$

$$C_D = 2.2 (V^2/ad)^{-1/2} \quad \text{eq (5)}$$

where

m_h = hydrodynamic mass

ρ = fluid density

d = disk diameter

V = peak harmonic velocity

a = peak harmonic acceleration

C_D = drag coefficient.

This is shown in figures 3 and 4.

The CABUOY program prints out the horizontal and vertical positions of the surface float and each cable node or body referenced to the surface float, their vertical and horizontal velocity and acceleration, their tilt angle from vertical, and the tension in the cable at the body for each point in time, spaced at user-selected time intervals.

VERTICAL MOTION VALIDATION MODEL

The primary experiment to evaluate the CABUOY vertical motion dynamics employed a body suspended from an elastic cable. The system was submerged in still fresh water in the Naval Surface Weapons Center (NAVSURFWPCEN) 100-foot deep Undersea Weapons Tank, as shown in figure 5. A rotating arm drive was used to produce a harmonic motion forcing function which translated to vertical motion by means of a pulley. Input amplitude and frequency could be varied at the motor. The motion of the body was viewed through portholes against a background grid recorded by an observer as well as photographed by a motion picture camera. In addition, a low frequency response pressure transducer system calibrated to give vertical amplitude of the body was recorded.

The bodies used were of three types, as shown in figure 6. A 3-inch high, 4-inch diameter aluminum cylinder weighing 4.24 lbs in air and 2.92 lbs in water was the basic body. To this, was, at times, attached a 12-inch diameter disk of 1/4-inch thick plexiglas (0.96 lbs in air, 0.16 lbs in water), a 12-inch diameter plastic flexible disk (of the type used in sonobuoy dampers, e.g., a spring steel hoop stretching taut a few mil thick plastic sheeting), and a pair of 12-inch plexiglas disks separated by 5-feet of inextensible line.

The elastic cable, or spring of this spring-mass system, was a 30-foot long piece of multistrand bungee of the type used in several sonobuoy systems. Typically, the bungee is a non-linear spring¹¹ and measurements of the bungee were made to characterize it for input to the computer program. The details of the bungee characterization will be discussed later. Initially, a simple stretching of the bungee was used to generate a tension-elongation plot as shown in figure 7.

SINGLE DISK SYSTEM

The single disk system (figure 6b) was selected as the first subject of comparison between measured behavior and computer predicted performance because the internal calculation of virtual mass could be utilized. The experimental data are shown in table I. Runs 6-12 used a rigid plexiglas disk and Runs 13-19 used a flexible plastic disk. No significant difference between the two disks were noted. Initial CABUOY outputs bore little resemblance to the experimental results. In an effort to determine why the computer results differed from empirical data, the program was modified to print out the body virtual mass and drag coefficient at each time interval in the output. The values that the program was calculating were not changing; they should have varied with the iterative process the CABUOY program was supposed to perform. The CABUOY generated values corresponded to

those expected at the limits placed upon the hydromechanical mass and drag coefficients of equations (4) and (5), i.e.,

$$0.08 \leq V^2/ad \leq 3.0. \quad \text{eq (6)}$$

The parameters V and a were apparently attaining values which would cause V^2/ad to achieve one of the limits.

The lower limit on V^2/ad is based on small amplitude vibration. In harmonic oscillation the peak velocity is the peak amplitude of motion, γ , multiplied by the angular frequency, ω :

$$V = \gamma\omega \quad \text{eq (7)}$$

and similarly

$$a = \gamma\omega^2 \quad \text{eq (8)}$$

therefore,

$$V^2/ad = \gamma^2\omega^2/\gamma\omega^2d = \gamma/d \quad \text{eq (9)}$$

The acceleration modulus V^2/ad is a measure of the amplitude of harmonic motion in disk diameters. At small amplitudes, the disk can be considered a vibrating circular piston in an infinite baffle¹² which for small amplitudes yields a hydrodynamic mass approaching

$$m_h = \frac{1}{3} \rho d^3. \quad \text{eq (10)}$$

This is the same value as the theoretical hydrodynamic mass from the kinetic energy imparted by a moving disk to an ideal, incompressible fluid of infinite extent as calculated by Milne-Thompson¹³.

As the amplitude of motion increases, a vortex ring which forms on the disk influences the hydrodynamic mass. At large amplitudes, the vortex sheds and the disk can be caused to skew to the side, "dumping" entrained water and confusing the dynamics to the point where repeatability is lost. This is the reason for the upper limit of V^2/ad . Even with these bounds, a 12-inch diameter disk should have its hydrodynamic mass defined by CABUOY for a peak-to-peak motion amplitude between 1.92 inches and 72.0 inches.

Removing the limits in the program did not resolve the problem. Further study of the CABUOY program uncovered a misinterpretation of V and a in the virtual mass calculation. Instantaneous values were being used instead of peak values. CABUOY was modified to retain maximum values for V and a over a time interval and use these values in recomputing the motion. This would be repeated during the next computation interval, and so on. This iterative technique finally resulted in a steady-state amplitude with consistent virtual mass calculations.

SPRING CHARACTERISTICS

The compliant cable used in most sonobuoy suspensions to isolate the sensor from the ocean wave effects on the surface float is a synthetic or natural rubber elastomer (or bungee cord). The bungee cord used in the validation testing was multistranded (9-strand) rubber with interwoven thread to provide a "haired-fairing" to reduce strumming in relative flow.

According to Hookes' Law,

$$T = k_s \Delta l = k_s (\ell - \ell_0) \quad \text{eq (11)}$$

where T is the force (tension) applied, ℓ is the stretched spring length under tension T, ℓ_0 is the unstretched spring length, and k_s is the (static) spring constant. The spring constant can be found by tensioning the spring by increasing amounts and measuring the resultant stretch. By setting elongation

$$\epsilon = \frac{\ell - \ell_0}{\ell_0} \quad \text{eq (12)}$$

$$T = (k_s \ell_0) \epsilon \quad \text{eq (13)}$$

which is the form of equation (1) where $k_s \ell_0 = C_1$, $T_{ref} = C_1 N T = 0$, and $C_2 = 1$. Because a bungee cord is not a linear spring but exhibits behavior like that shown in figure 2, a portion can be linearized around the operating point by using equation (1). This is shown graphically in figure 7 for the multistrand bungee used.

Another way of determining a spring constant is through the solution to the equation of motion of an undamped spring-mass system:

$$\ddot{m}y + ky = 0 \quad \text{eq (14)}$$

The solution to this equation is

$$y = y_0 \sin \omega t \quad \text{eq (15)}$$

where y_0 is the peak amplitude of motion, t is time, and ω is the angular frequency. The natural frequency is

$$\omega_n = \sqrt{k_d/m} \quad \text{eq (16)}$$

where k_d is the (dynamic) spring constant and m is the mass of body on the end of the spring. In an ideal spring,

$$k_s = k_d; \quad \text{eq (17)}$$

however, this is not true for the bungee cord. When masses of different weight were hung upon a sample of the bungee and the natural frequency measured, k_d was found for the range of loads on the cable. This is shown in figure 8 in comparison with k_s measured from the static stretch of the bungee.

The linear static equation (as shown in figure 7) which satisfies the form of the CABUOY program (eq (1)) in the operating range of loads (static load 2.9 to 3.1 lbs) is

$$T = 1.08 + 1.05 \epsilon \quad \text{eq (18)}$$

In obtaining this equation, a graphical method was used as illustrated in figure 2. A similar equation for the dynamic properties of the bungee can be devised. The derivation of that equation is explained as follows:

The static spring constant k_s is defined as

$$k_s = \frac{T_s}{l_s - l_0} \quad \text{eq (19)}$$

where T_s is the static tension, l_0 is the unstretched length of the spring, and l_s is the stretched length under static tension, T_s . This can be written as

$$l_0 k_s = T_s / \epsilon_s \quad \text{eq (20)}$$

where

$$\epsilon_s = \frac{l_s - l_0}{l_0} \quad \text{eq (21)}$$

The non-linear bungee has a linear range described by the equation

$$T_s = T_{ref} + C_1 \epsilon_s \quad \text{eq (22)}$$

Combining this with equation (20),

$$l_0 k_s \epsilon_s = T_{ref} + C_1 \epsilon_s \quad \text{eq (23)}$$

$$C_1 = l_0 k_s - T_{ref} / \epsilon_s \quad \text{(eq (24))}$$

The dynamic spring constant can be defined¹⁴ as

$$k_d = \frac{\Delta T}{\Delta l} = \frac{T - T_s}{l - l_s} \quad \text{eq (25)}$$

where T is the tension and l is the length of the spring displaced from the static position. The tension can be expressed as

$$T = T_s + k_d (l - l_s) \quad \text{eq (26)}$$

Since

$$l - l_0 = (l - l_s) + (l_s - l_0) \quad \text{eq (27)}$$

equation (26) can be rewritten as

$$T = T_s + k_d (l - l_0) - k_d (l_s - l_0) \quad \text{eq (28)}$$

Using equation (22) to substitute for T_s ,

$$T = T_{ref} + C_1 \epsilon_s + k_d (l - l_0) - k_d (l_s - l_0) \quad \text{eq (29)}$$

Substituting equation (24),

$$T = T_{ref} + l_0 k_s \epsilon_s - T_{ref} + k_d (l - l_0) - k_d (l_s - l_0) \quad \text{eq (30)}$$

or

$$T = l_0 k_s \epsilon_s + k_d (l - l_0) - k_d (l_s - l_0). \quad \text{eq (31)}$$

Using equation (21) and rearranging,

$$T = k_s (l_s - l_0) - k_d (l_s - l_0) + k_d (l - l_0) \quad \text{eq (32)}$$

$$T - (k_s - k_d) (l_s - l_0) + k_d (l - l_0). \quad \text{eq (33)}$$

Multiplying by l_0/l_0 ,

$$T = (k_s - k_d) (l_s - l_0) + l_0 k_d \frac{l - l_0}{l_0} \quad \text{eq (34)}$$

This is of the form of

$$T = T_{ref} + C_1 \epsilon \quad \text{eq (35)}$$

where

$$C_1 = l_0 k_d \quad \text{eq (36)}$$

$$\epsilon = \frac{l - l_0}{l_0} \quad \text{eq (37)}$$

and

$$T_{ref} = (k_s - k_d) (l_s - l_0) \quad \text{eq (38)}$$

which by using equation (19) reduces to

$$T_{ref} = (k_s - k_d) \frac{l_s}{k_s} = T_s \left(1 - \frac{k_d}{k_s} \right) \quad \text{eq (39)}$$

The dynamic equation to be used in CABUOY is then equation (35) with the constants and parameters defined in equations (36), (37), and (39). For the multistrand bungee where $l_0 = 30$ ft, at $T_s = 2.9$ lbs, $k_s \approx 0.0567$ and $k_d \approx 0.0425$ and equation (35) becomes

$$T = 0.75 + 1.27 \epsilon \quad \text{eq (40)}$$

A comparison between the dynamic and static expressions describing the cable is shown in figure 9. Both lines go through the static operating point, but have different slopes. Both equation (18) and equation (40) were used in CABUOY to describe the bungee and the results compared with observed data, as shown in table 11 and figure 10. The dynamic spring equation produced slightly better results than the static equation. The CABUOY results using the dynamic spring characterization were consistent with consistently lower amplitudes than the observed values. A maximum error of 20% was observed but most calculated data were within 12% of the observed results except

at small amplitudes where the largest experimental percentage errors occurred. In absolute terms, the error amounted to approximately 4 inches in 34 inches, 2.5 inches in 13 inches, and 0.5 inches in 1.5 inches, while the visual observations had probable errors of ± 1.5 inches.

AMPLITUDE VARIATION

A phenomenon observed in the past was noted in the vertical motion experiments. When comparing the magnification factor (i.e., output amplitude/input amplitude) of the same system with two different input amplitudes, the magnification factor of the smaller input was larger. The disk system with a 3-foot input amplitude (table III) was compared with the 6-foot input data (table I) with similar results. Table IV shows the CABUOY calculated amplitudes for the 3-foot input, and figure 11 shows the comparison of observed and calculated data for the 3-foot and 6-foot input cases. The magnification factor for the CABUOY calculations follows the form of the observed data closely.

Figure 12 compares the CABUOY calculated data for both amplitude inputs to the disk system to observed data. If the maximum error in observation is ± 1.5 inches, the calculated data falls within the envelope of expected values only if an offset in the calculation is taken into account. The calculated values are apparently 10% lower than the experimental data. This is probably a function of the coefficients used in the virtual mass and drag equations for the disk. An area for further investigation might be in varying these coefficients for improved agreement with the observed data.

TWO DISK SYSTEM

The two-disk system (figure 6c) was oscillated with a 3-foot input amplitude vertical motion on the 30-foot bungee. The disks were separated by 5 feet of non-compliant line. Observed and calculated data are shown in table V. Each disk was considered as a separate body in the CABUOY simulation with independently calculated virtual masses (i.e., assuming no interference effects), as predicted by reference 10 for this separation.

The results show excellent agreement with observations, better than the single disk system. A comparison between the single and dual disk systems with the same input amplitude is shown in figure 13.

CYLINDER SYSTEM

The 3-inch high, 4-inch diameter cylinder in figure 6a was oscillated on the end of the 30-foot bungee with both 3-foot and 6-foot peak-to-peak input amplitudes. The CABUOY program can internally calculate the virtual mass and drag associated with an oscillating disk in the form of equations (4) and (5). Figures 14 and 15 show the drag and virtual mass for oscillating cylinders over a limited range of length-to-diameter ratios.¹⁰ Since the cylinder used in the experiments had an ℓ/d ratio of 0.75, the disk-type drag (see figure 14) could be used, but a modification to the virtual mass equation used in the CABUOY program was required, since the internal virtual mass calculations were originally only defined for disks.

The hydrodynamic mass for the cylinder in figure 15 is in the form

$$m_h = C_l \rho \frac{\pi}{4} d^2 \ell \quad \text{eq (41)}$$

Rather than to introduce a new set of equations into CABUOY, the form of equation (4) was used:

$$m_h = C_l \rho \frac{\pi}{4} d^2 \ell = C_l^* \rho d^3 (V^2/ad)^{1/2} \quad \text{eq (42)}$$

or

$$C_l^* = \frac{\pi}{4} \left(\frac{\ell}{d} \right) C_l (V^2/ad)^{-1/2} \quad \text{eq (43)}$$

For $\ell/d = 0.75$,

$$C_l^* = 0.589 C_l (V^2/ad)^{-1/2} \quad \text{eq (44)}$$

Using figure 15, values for C_l and V^2/ad were found to yield an approximate solution $C_l^* = 0.55$, for $\ell/d = 0.75$. This was used in place of the 1.2 value in equation (4) and the output data compared with observed data in figure 16 and table VI. The agreement between the calculated and observed data is not as good as that for the disk system but is certainly a useful approximation.

It was beyond the scope of the present study to extend the virtual mass data for oscillating cylinders, but it became obvious that the validity of the computer solutions are dependent on this data. A preliminary graph of the hydrodynamic mass coefficient C_l^* in the equation

$$m_h C_l^* \rho d^3 (V^2/ad)^{1/2} \quad \text{eq (45)}$$

for low ℓ/d cylinders is shown in figure 17, based on the curves in figure 15. An approximation for drag coefficient for $0.8 < \ell/d < 2$ may be used as follows:

$$C_D = 0.83 + 0.25 (V^2/ad)^{-1/2} \quad \text{eq (46)}$$

whereas for $\ell/d < 0.75$, the disk formulation can be used for drag.

ACKNOWLEDGEMENT

The author wishes to thank T. Kraynak, T. DeDominicis, M. Snyderwine, and J. Yocom for their contributions in both the experimental and computational phases of the validation effort. He also wishes to acknowledge the indispensable contributions of Mr. John Brett and Dr. Henry Wang in the seemingly endless process of updating and upgrading the CABUOY program, both past and present.

REFERENCES

1. Wang, H. T., "Preliminary Report on a Fortran IV Computer Program for the Two-Dimensional Dynamic Behavior of General Ocean Cable Systems," NAVSHIPRANDCEN Report SPD-633-01, Aug 1975.
2. Wang, H. T., "A Fortran IV Computer Program for the Time Domain Analysis of the Two-Dimensional Dynamic Motions of General Buoy - Cable-Body Systems," NAVSHIP-RANDCEN Report 77-0046, June 1977.
3. Wang, H. T., "Technique for Efficient Time-Domain Analysis of Complete Buoy-Cable Systems," Trans. ASME Vol. 101, pp 416-420, Nov 1979.
4. Wang, H. T., "Description of the Revised Buoy-Cable-Body Computer Program CABMOD," DTNAVSHIPRANDECEN Report SPD-0633-02, Aug 1978.
5. Brett, J. P., "Computer Generated Random Sea Surfaces for use with the Program CABUOY," NAVAIRDEVCCEN Report NADC-77271-20, Sep 1977.
6. Brett, J. P., "User's Manual for the Buoy-Cable-Body Computer Program CABUOY," NAVAIRDEVCCEN Report NADC-80174-30, Sep 1981.
7. Wang, H. T., and Cheng, R. S., "Description of Computer Program CAB3DYN for the Time Domain Analysis of the Three-Dimensional Long-Time Deployment Behavior of General Ocean Cable Systems," DTNAVSHIPRANDCEN Report SPD-0633-30, Dec 1981.
8. Wang, H. T. and Moran, T. L., "Analysis of the Two Dimensional Steady State Behavior of Extensible Free-Floating Cable Systems," DTNAVSHIPRANDCEN Report 3721, Oct 1971.
9. Wang, H. T., "Effect of Nonplanar Current Profiles on the Configuration of Moored Cable Systems," DTNAVSHIPRANDCEN Report 3692, Oct 1971.
10. Holler, R. A., "Hydrodynamic Effects of Harmonic Acceleration," NAVAIRDEVCCEN Report NADC-AE-7120, Jan 1982.
11. Brett, J. P., "Nonlinear Variations in Effective Spring Constants of Bungee Cords," NAVAIR-DEVCCEN (Code 3043) Technical Memorandum 2063-TM-11-74, Feb 1974.
12. Kinsler, L., and Frey, A. R.; Fundamentals of Acoustics; John Wiley and Sons, Inc., New York, c. 1950.
13. Milne-Thompson, Lm M.; Theoretical Hydrodynamics; The MacMillan Company; New York, 1950.
14. Cormier, D. R., and Scheiber, D. J., "Measurements of the Dynamic Properties of a Compliant Cable," The Magnavox Company, Report MX-TR-6-7-200166, Nov 1966.

NADC 83112-30

TABLE I - EXPERIMENTAL DATA FOR 12-INCH DIAMETER DISK ON 30-FEET LENGTH OF BUNGEE. (RUNS 6-12 FOR PLEXIGLAS (RIGID) DISK, RUNS 13-19 FOR PLASTIC (FLEXIBLE) DISK) WITH 6-FEET INPUT AMPLITUDE.

RUN	PERIOD (sec)	FREQUENCY (Hz)	INPUT AMPLITUDE PEAK-TO-PEAK (ft)	OUTPUT AMPLITUDE PEAK-TO-PEAK (ft)	MAGNIFICATION FACTOR yout/yin
6	3.6	0.278	6.00	0.125	0.021
7	5.0	0.200	6.00	0.250	0.042
8	8.0	0.125	6.00	0.474	0.079
9	12.3	0.081	6.00	0.639	0.107
10	14.9	0.067	6.00	1.062	0.177
11	19.6	0.051	6.00	1.437	0.240
12	30.3	0.033	6.00	2.811	0.469
13	3.6	0.278	6.00	0.114	0.019
14	5.3	0.188	6.00	0.182	0.030
15	8.0	0.125	6.00	0.400	0.067
16	12.0	0.083	6.00	0.692	0.115
17	15.9	0.063	6.00	1.120	0.187
18	22.7	0.044	6.00	1.832	0.305
19	30.3	0.033	6.00	2.744	0.457

NADC-83112-30

TABLE II – COMPARISON OF CABUOY CALCULATED OUTPUT USING STATIC AND DYNAMIC SPRING EQUATIONS WITH OBSERVED AMPLITUDE MEASUREMENTS FOR THE DISK SYSTEM (6-FEET INPUT AMPLITUDE).

RUN	FREQUENCY (Hz)	OBSERVED OUTPUT (ft)	STATIC SPRING EQUATION CALCULATED OUTPUT (ft)	DYNAMIC SPRING EQUATION CALCULATED OUTPUT (ft)
6	0.278	0.125	0.09	0.08
7	0.200	0.250	0.16	0.16
8	0.125	0.474	0.34	0.34
9	0.081	0.639	0.63	0.63
10	0.067	1.062	0.83	0.85
11	0.051	1.437	1.24	1.27
12	0.033	2.811	2.39	2.49
13	0.278	0.114	0.10	0.10
14	0.188	0.182	0.19	0.20
15	0.125	0.400	0.34	0.34
16	0.083	0.692	0.61	0.63
17	0.063	1.120	0.92	0.93
18	0.044	1.832	1.56	1.60
19	0.033	2.744	2.41	2.51

TABLE III – EXPERIMENTAL DATA FOR 12-INCH DIAMETER DISK ON 30-FEET BUNGEE WITH 3-FEET INPUT AMPLITUDE.

RUN	PERIOD (sec)	FREQUENCY (Hz)	INPUT	INPUT	MAGNIFICATION FACTOR yout/yin
			AMPLITUDE p-p (ft)	AMPLITUDE p-p (ft)	
27	3.5	0.286	3.00	0.075	0.025
28	6.0	0.167	3.00	0.140	0.047
29	10.0	0.100	3.00	0.321	0.107
30	15.0	0.067	3.00	0.576	0.192
31	20.0	0.050	3.00	0.885	0.295
32	30.0	0.033	3.00	1.749	0.583

NADC-83112-30

TABLE IV – COMPARISON OF CABUOY CALCULATED OUTPUT (USING DYNAMIC SPRING EQUATION) WITH OBSERVED MEASUREMENTS FOR DISK SYSTEM (3-FOOT INPUT AMPLITUDE).

RUN	FREQUENCY (Hz)	OBSERVED OUTPUT	CALCULATED OUTPUT
		p-p (ft)	p-p (ft)
27	0.286	0.075	0.050
28	0.167	0.140	0.140
29	0.100	0.321	0.300
30	0.067	0.0576	0.520
31	0.050	0.885	0.820
32	0.033	1.749	1.640

TABLE V – COMPAIRSON OF CABUOY CALCULATED OUTPUT WITH OBSERVED MEASUREMENTS FOR A TWO-DISK SYSTEM.

RUN	PERIOD (sec)	FREQUENCY (Hz)	INPUT AMPLITUDE	OBSERVED OUTPUT AMPLITUDE	CALCULATED OUTPUT AMPLITUDE
			p-p (ft)	p-p (ft)	p-p (ft)
33	4.0	0.250	3.00	0.063	0.050
34	7.5	0.133	3.00	0.126	0.130
35	13.0	0.077	3.00	0.264	0.260
36	23.0	0.043	3.00	0.611	0.590
37	30.0	0.033	3.00	0.990	0.960

NADC-83112-30

TABLE VI - COMPARISON OF OBSERVED AND CABUOY CALCULATED MOTION OF A CYLINDRICAL WEIGHT (L/D = 0.75) ON THE 30-FEET LENGTH OF BUNGEE.

RUN	PERIOD (sec)	FREQUENCY (Hz)	INPUT	OBSERVED	CALCULATED	OBSERVED
			AMPLITUDE p-p (ft)	OUTPUT AMPLITUDE p-p (ft)	OUTPUT AMPLITUDE p-p (ft)	MAGNIFICATION FACTOR (yout/yin)
1	30	0.033	6.0	7.00	7.36	1.167
2	15	0.067	6.0	5.06	5.96	0.843
3	8	0.125	6.0	2.42	2.42	0.403
4	5	0.200	6.0	1.07	0.97	0.178
5	3.5	0.296	6.0	0.50	0.55	0.083
20	4	0.250	3.0	0.25	0.22	0.083
21	5	0.200	3.0	0.62	0.61	0.207
22	8	0.125	3.0	1.37	1.46	0.457
23	12.5	0.080	3.0	2.50	3.22	0.833
24	16	0.0625	3.0	3.25	4.22	1.083
25	23	0.435	3.0	3.75	4.25	1.250
26	30	0.033	3.0	3.75	3.80	1.250

CABUOY
MODEL DEFINITION

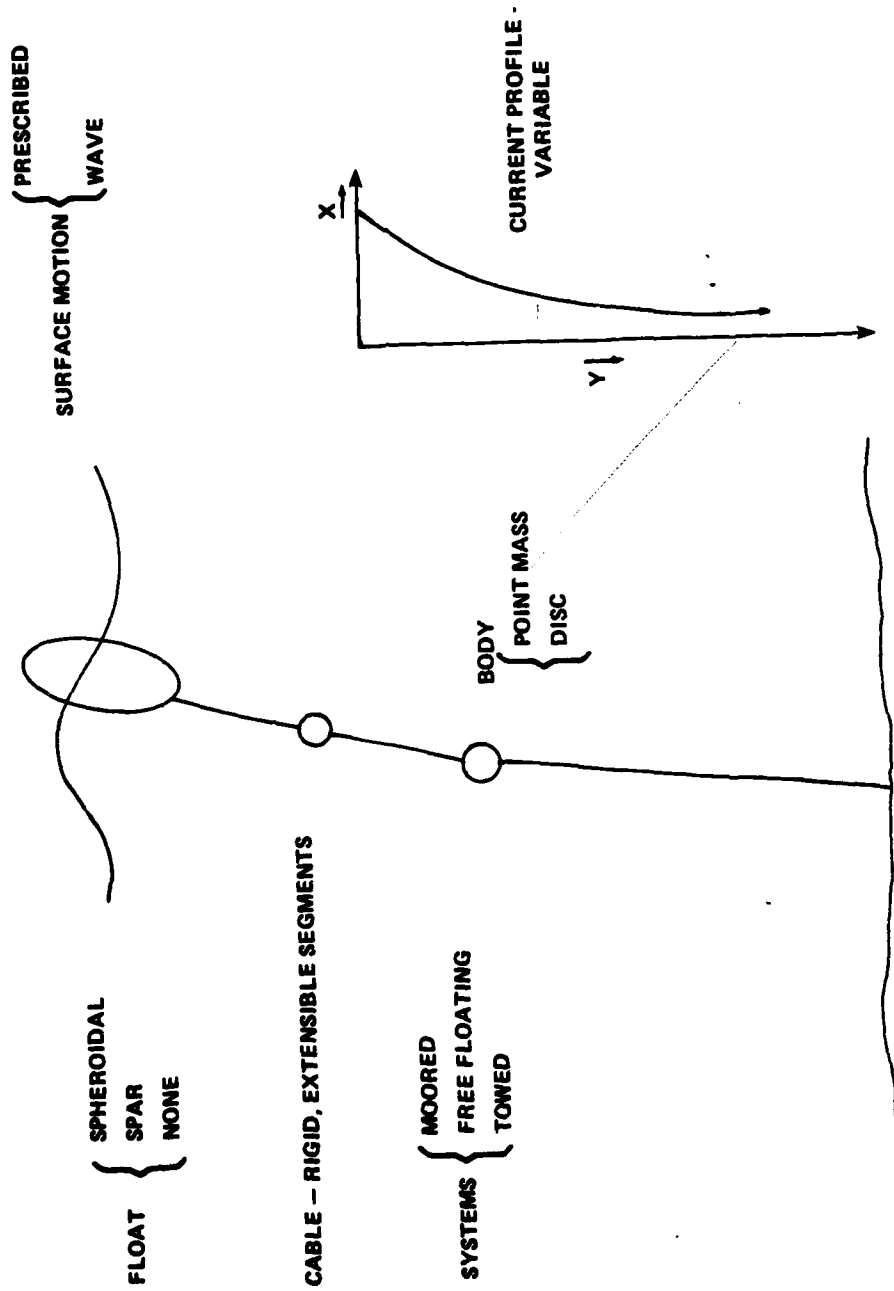


Figure 1. CABUOY (Model Definition).

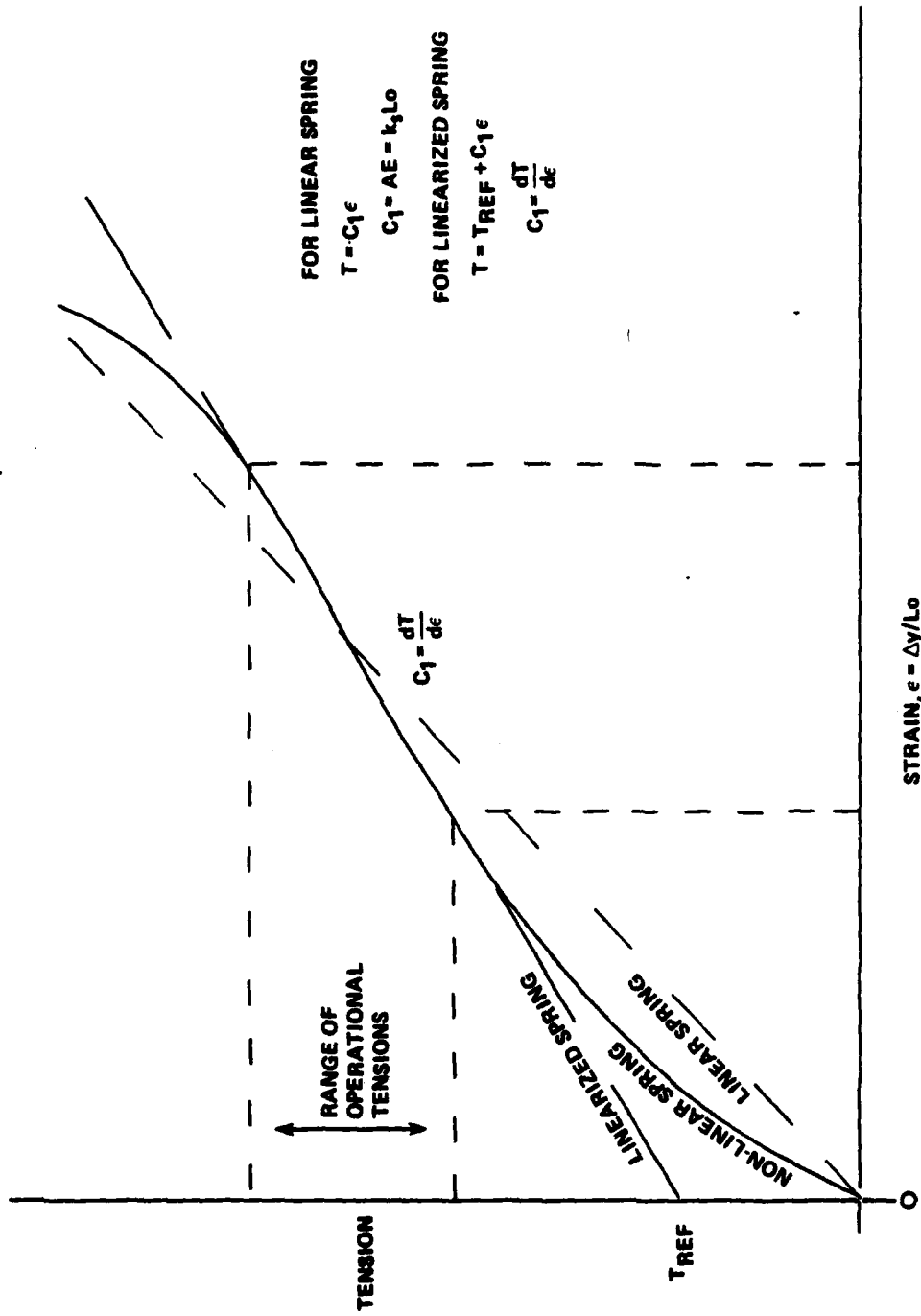


Figure 2. Linearization Of Bungee Stress-Strain Curve.

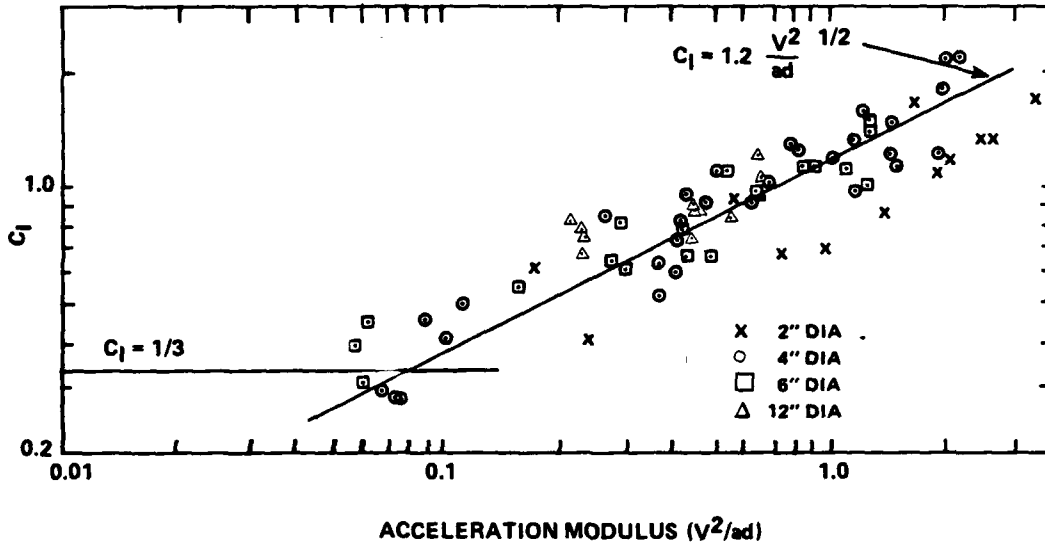


Figure 3. Hydrodynamic Inertia Coefficient Versus Acceleration Modulus For Oscillating Disks ($C_I = m_H/\rho d^3$).

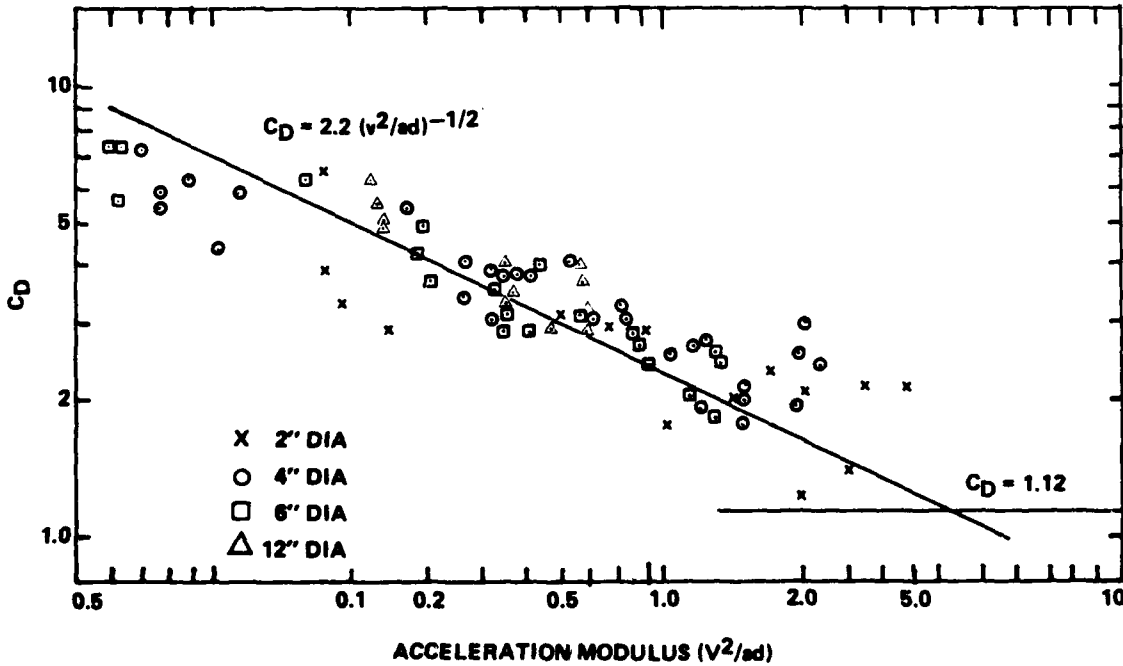


Figure 4. Drag Coefficient Versus Acceleration Modulus For Oscillating Disks.

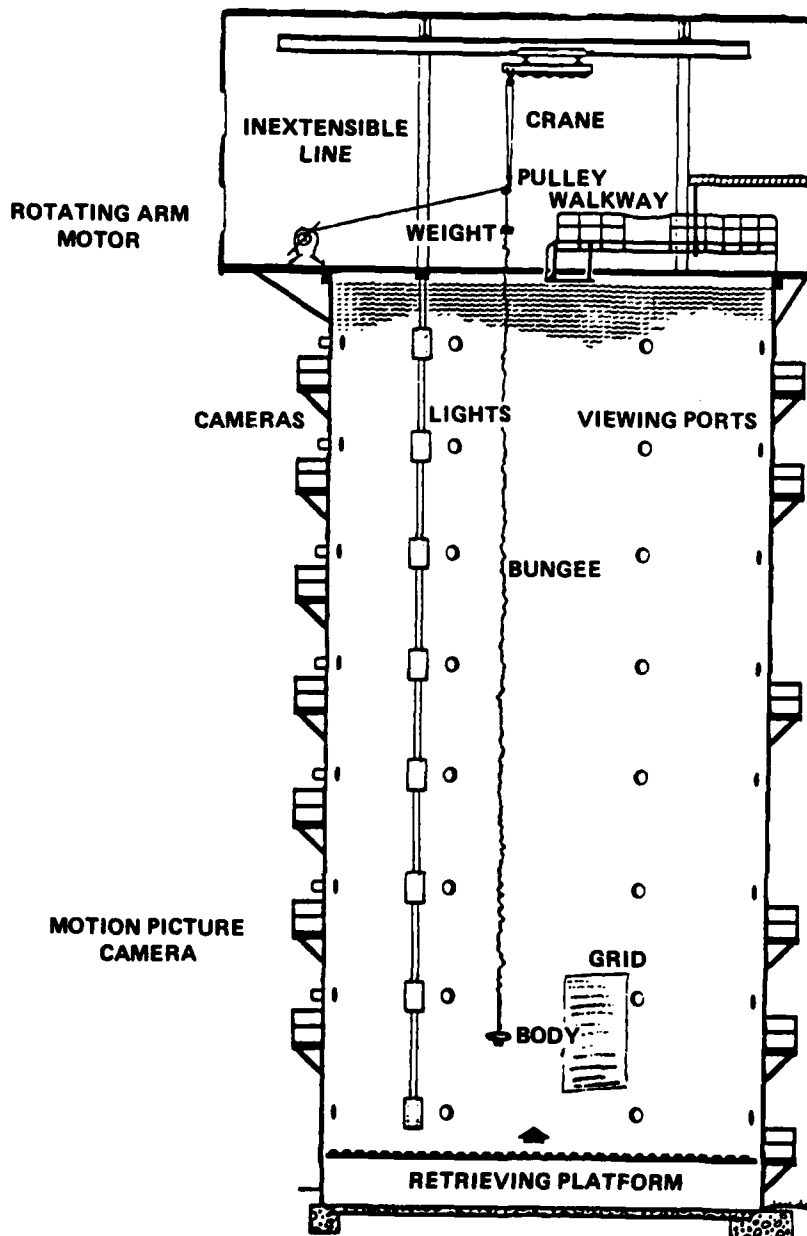


Figure 5. Vertical Motion Experimental Arrangement In The 100-Foot NAVSURFWPNCEN Undersea Weapons Tank.

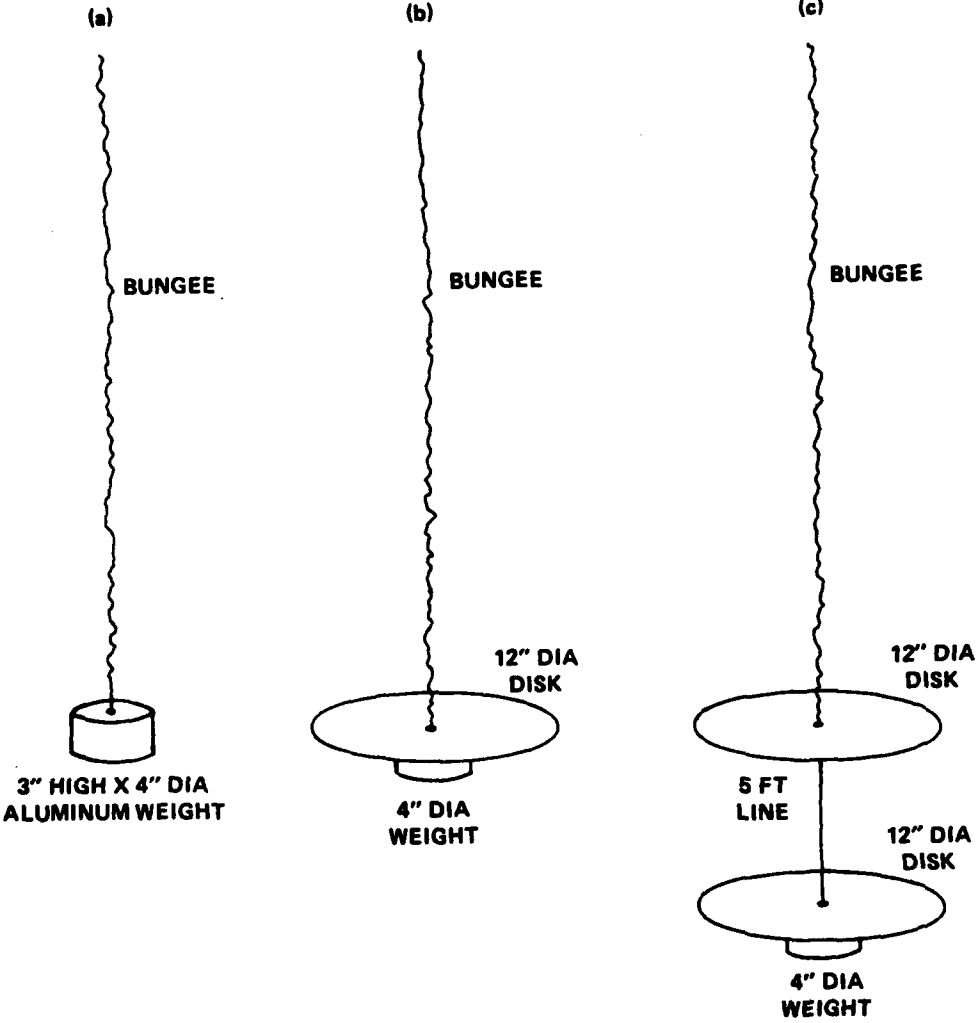


Figure 6. Three Body Types Used in The NAVSURFWPNCEN 100-Foot Tank Experiment.

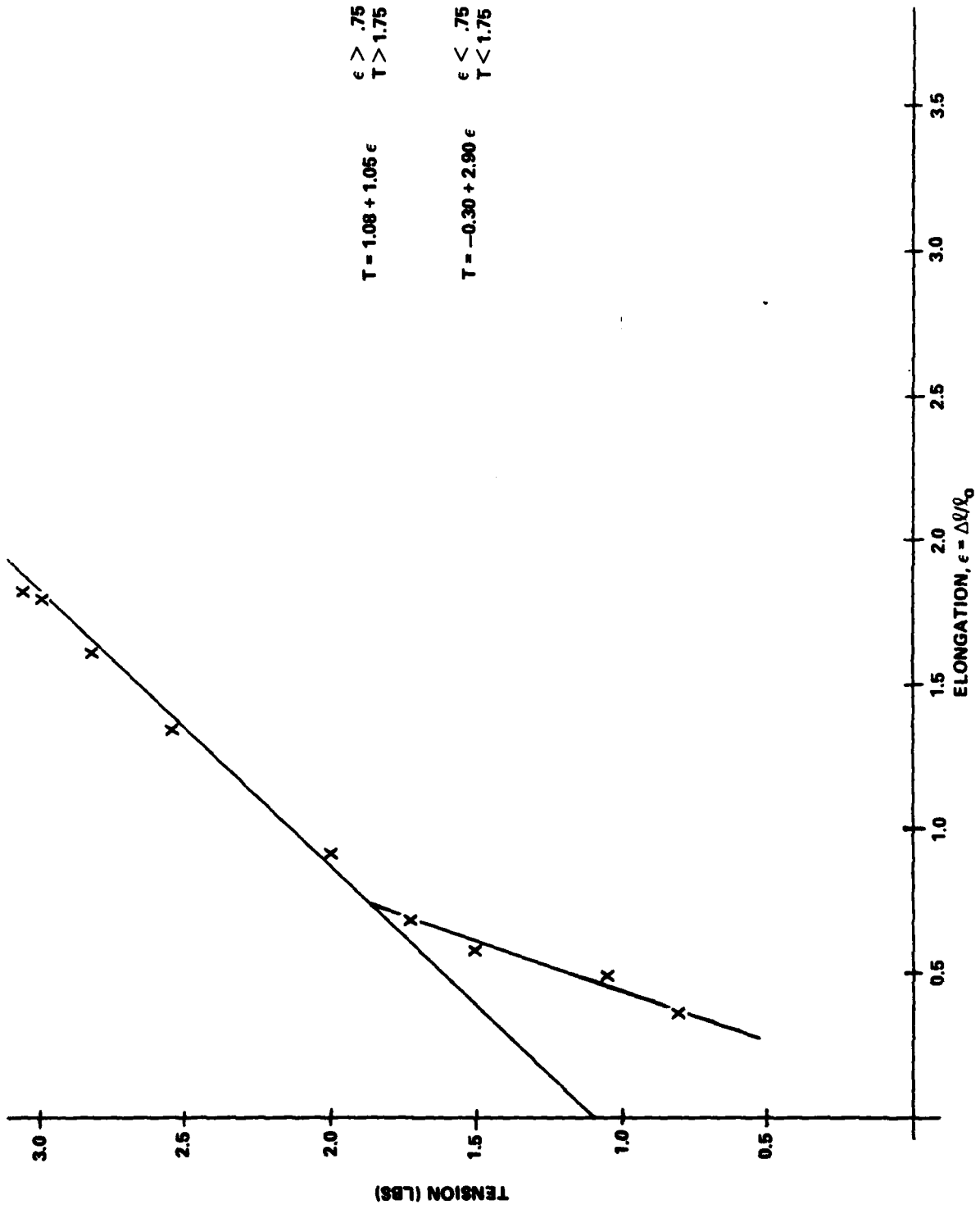


Figure 7. Elongation Of The Multistrand Bungee Under Static Tension.

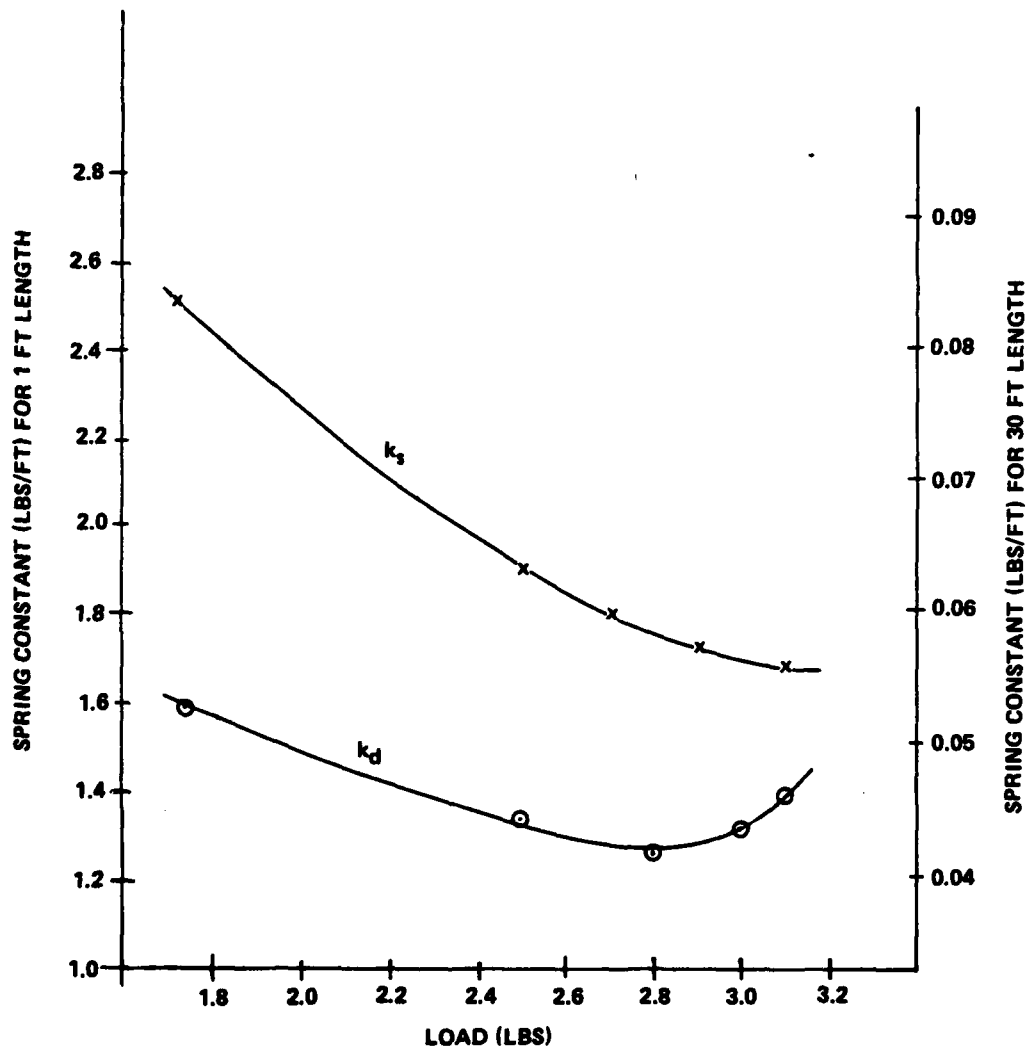


Figure 8. Static And Dynamic Spring Constants For Multistrand Bungee Under Load.

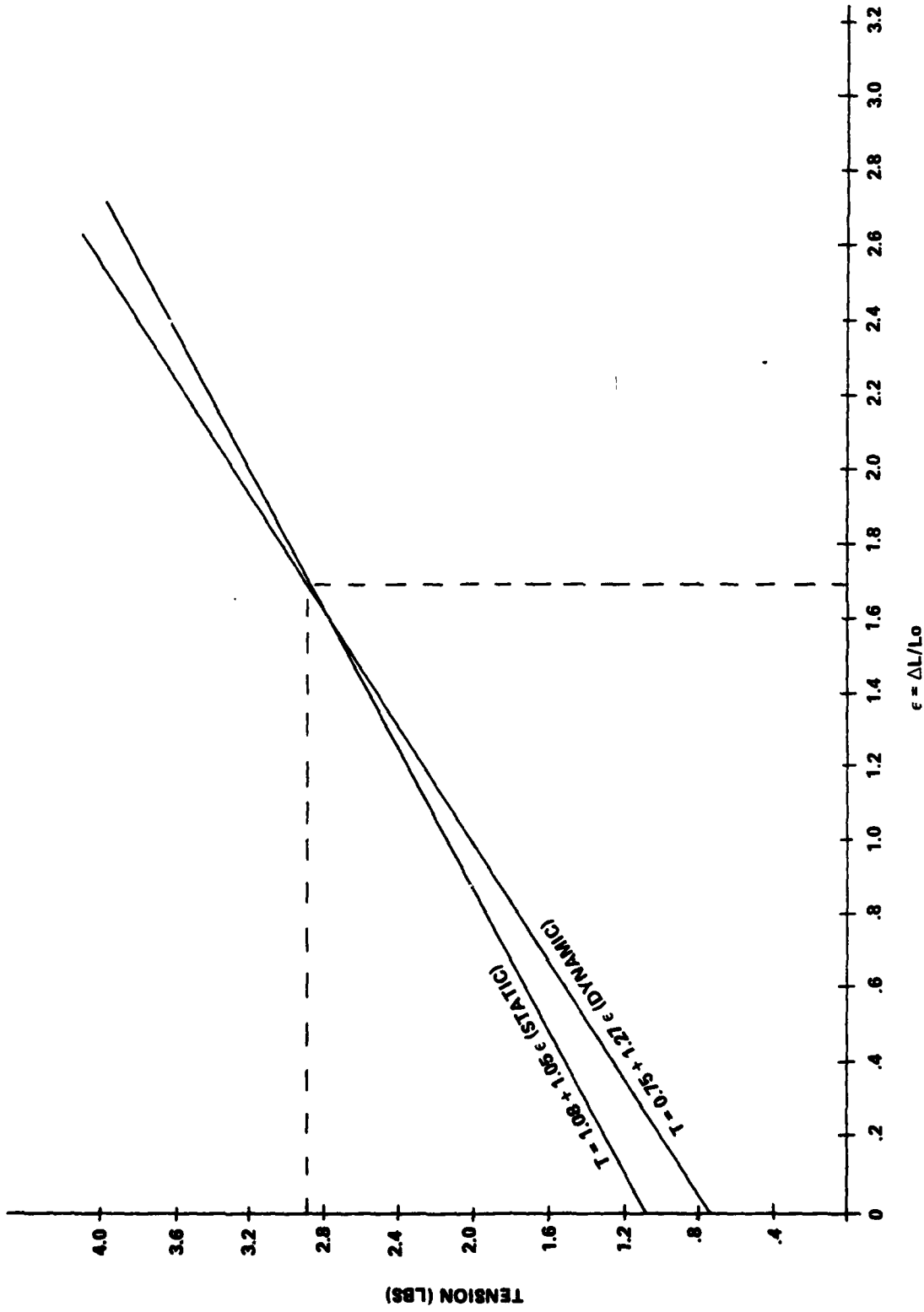


Figure 9. Comparison Of Dynamic And Static Equations To Characterize The Multistrand Bungee.

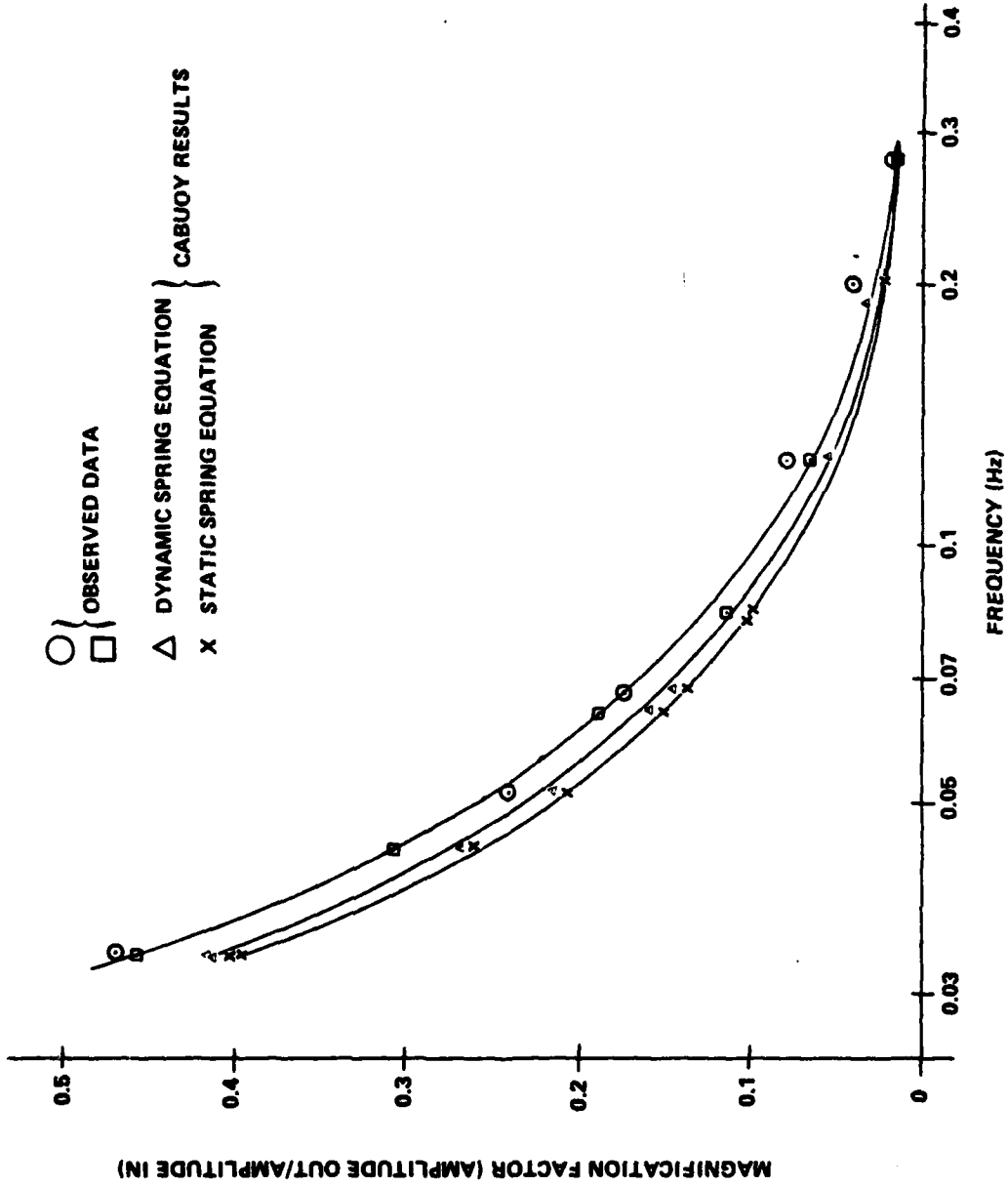


Figure 10. Comparison Of CABUOY Results With Observed Measurements For The Disk System (30-Foot Compliance, 6-Foot p-p Input Amplitude).

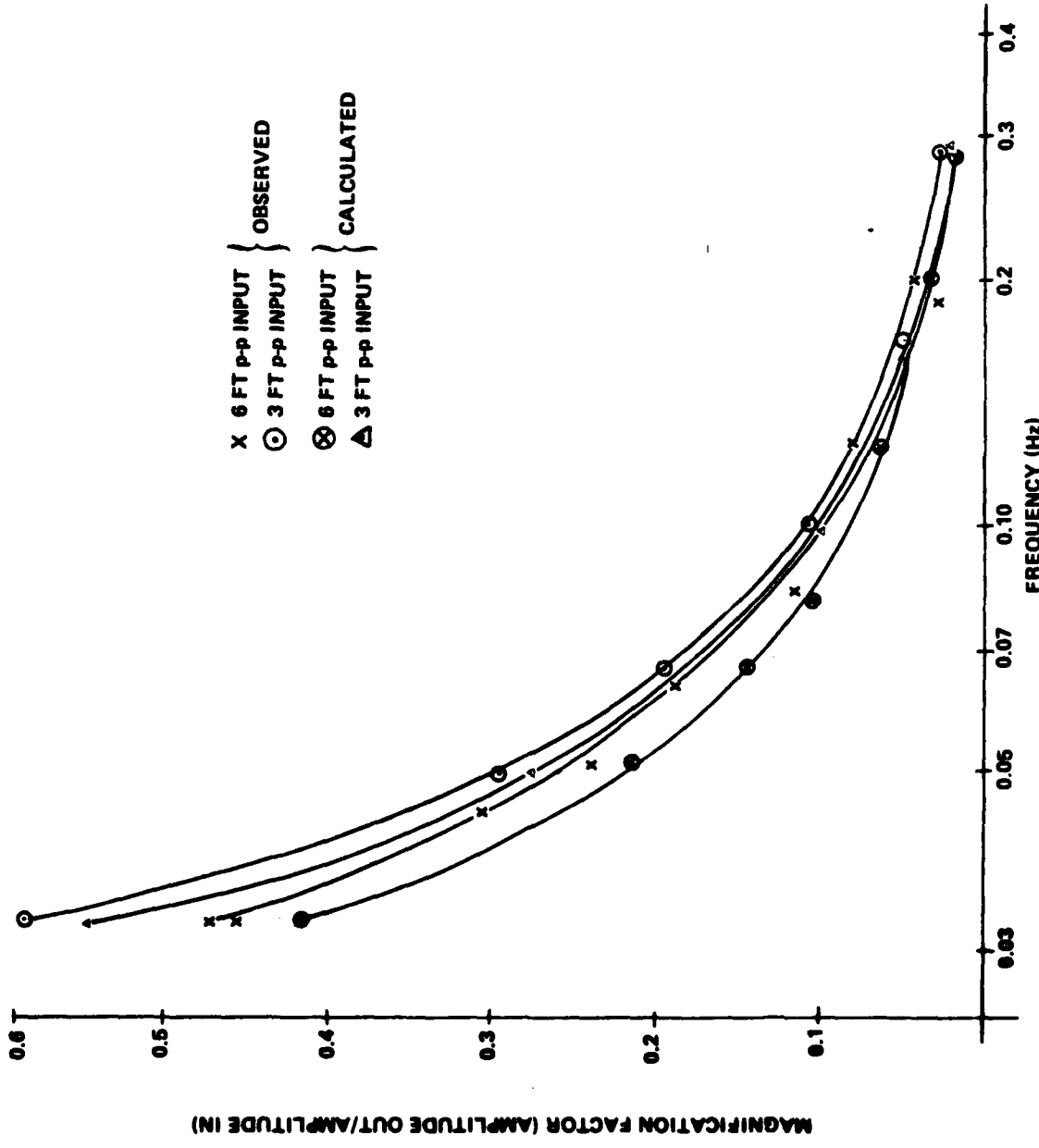


Figure 11. Comparison Of Observed And CABUOY Results For The Disk System (30-Foot Compliance) With 3-Foot And 6-Foot p-p Input Amplitudes.

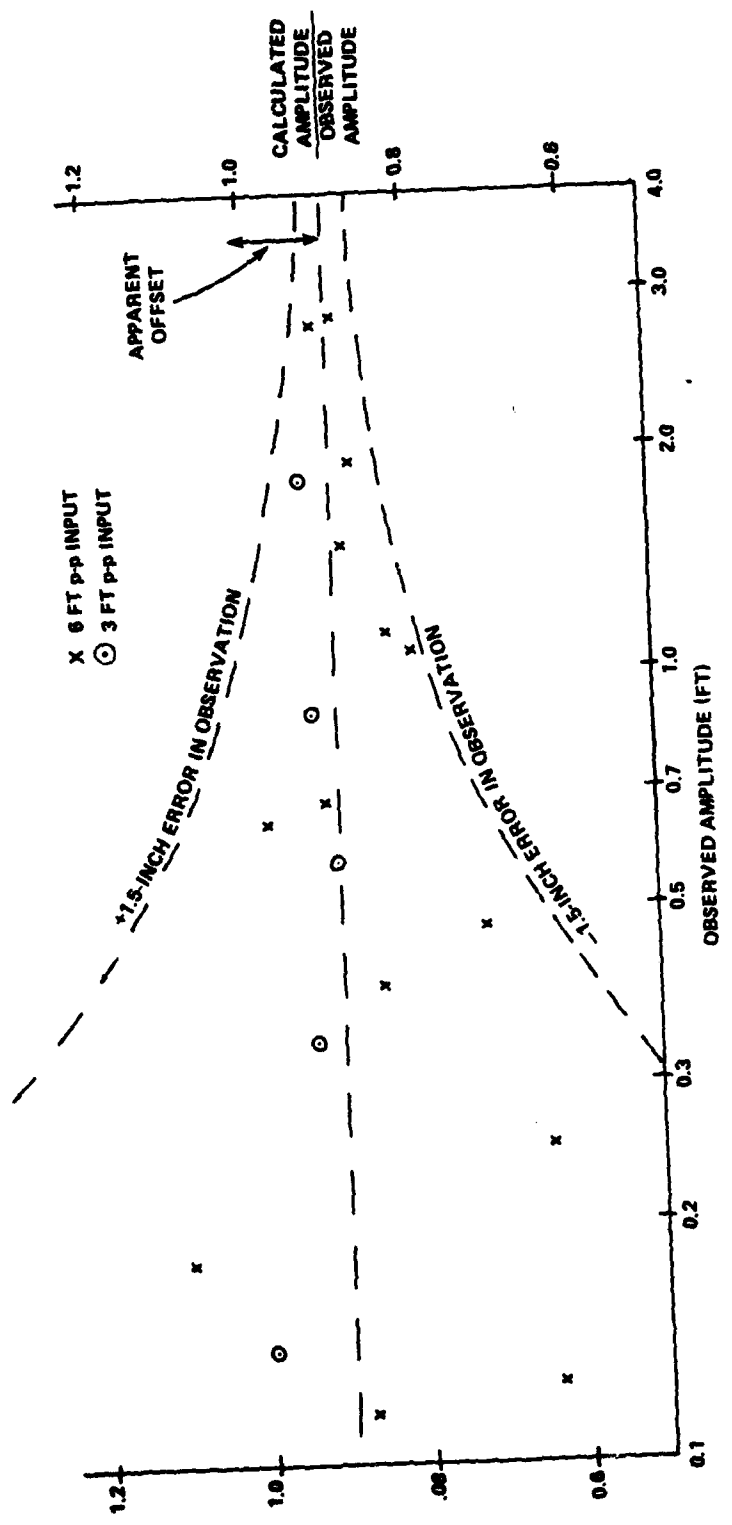


Figure 12. Comparison Of Calculated Data On Disk System And Observed Data As A Function Of Observed Amplitude.

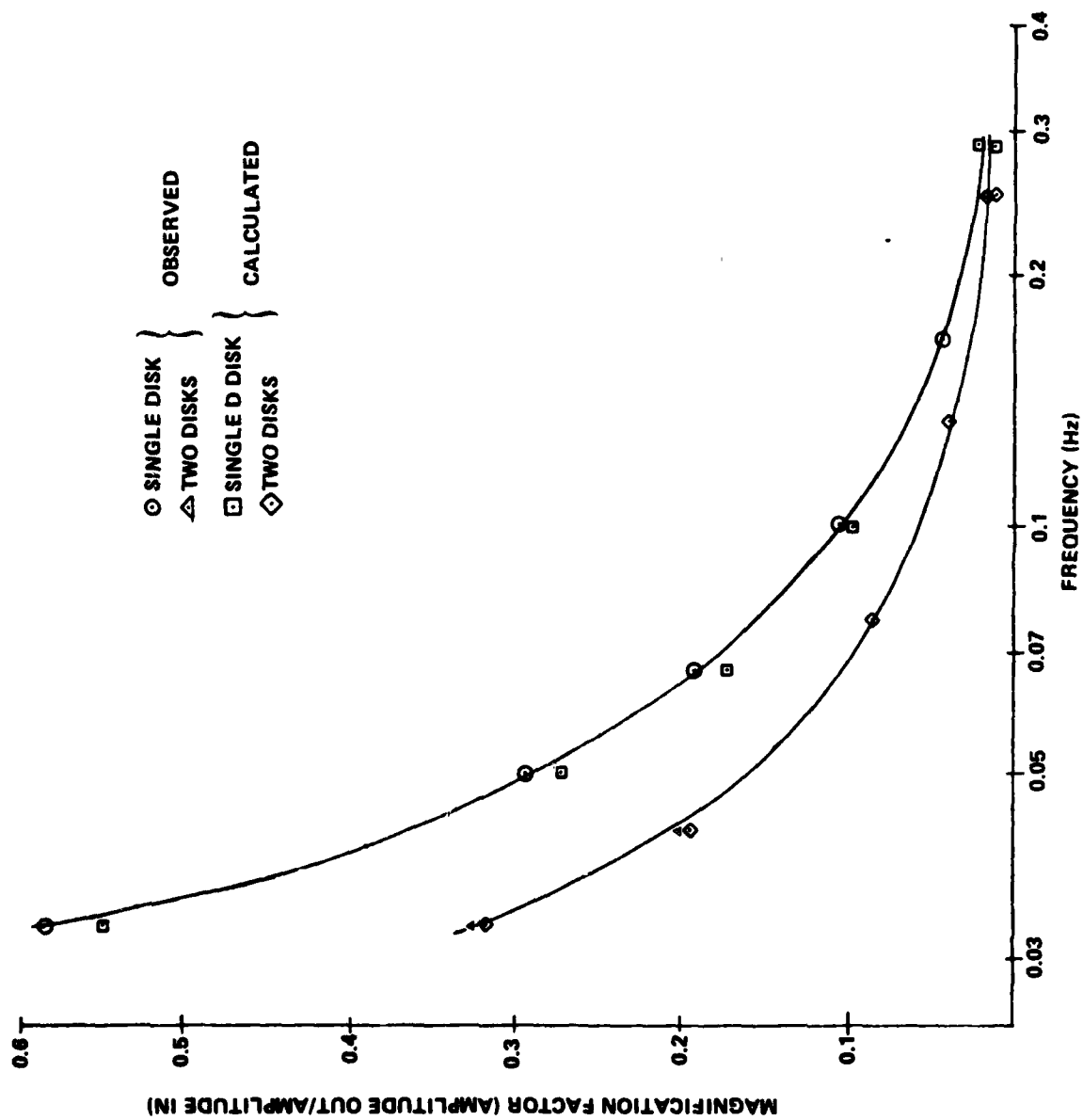


Figure 13. Comparison Of Single Disk And Two Disk Systems With 3-Foot p-p Input Amplitude (30-Foot Bungee).

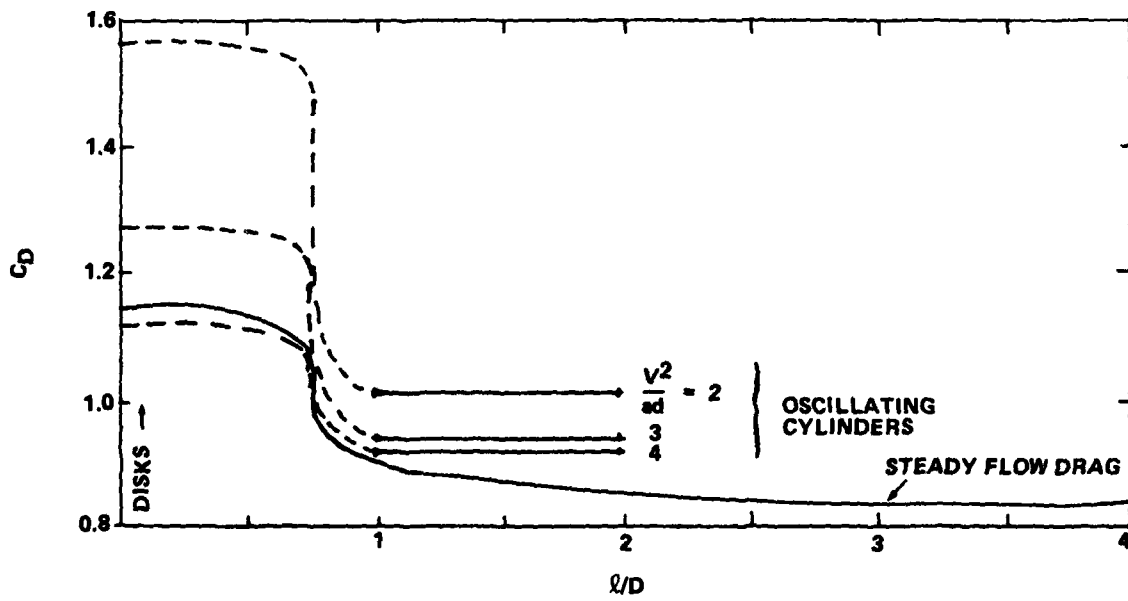


Figure 14. Drag Coefficient Versus Length-To-Diameter Ratio For Oscillating Cylinders.

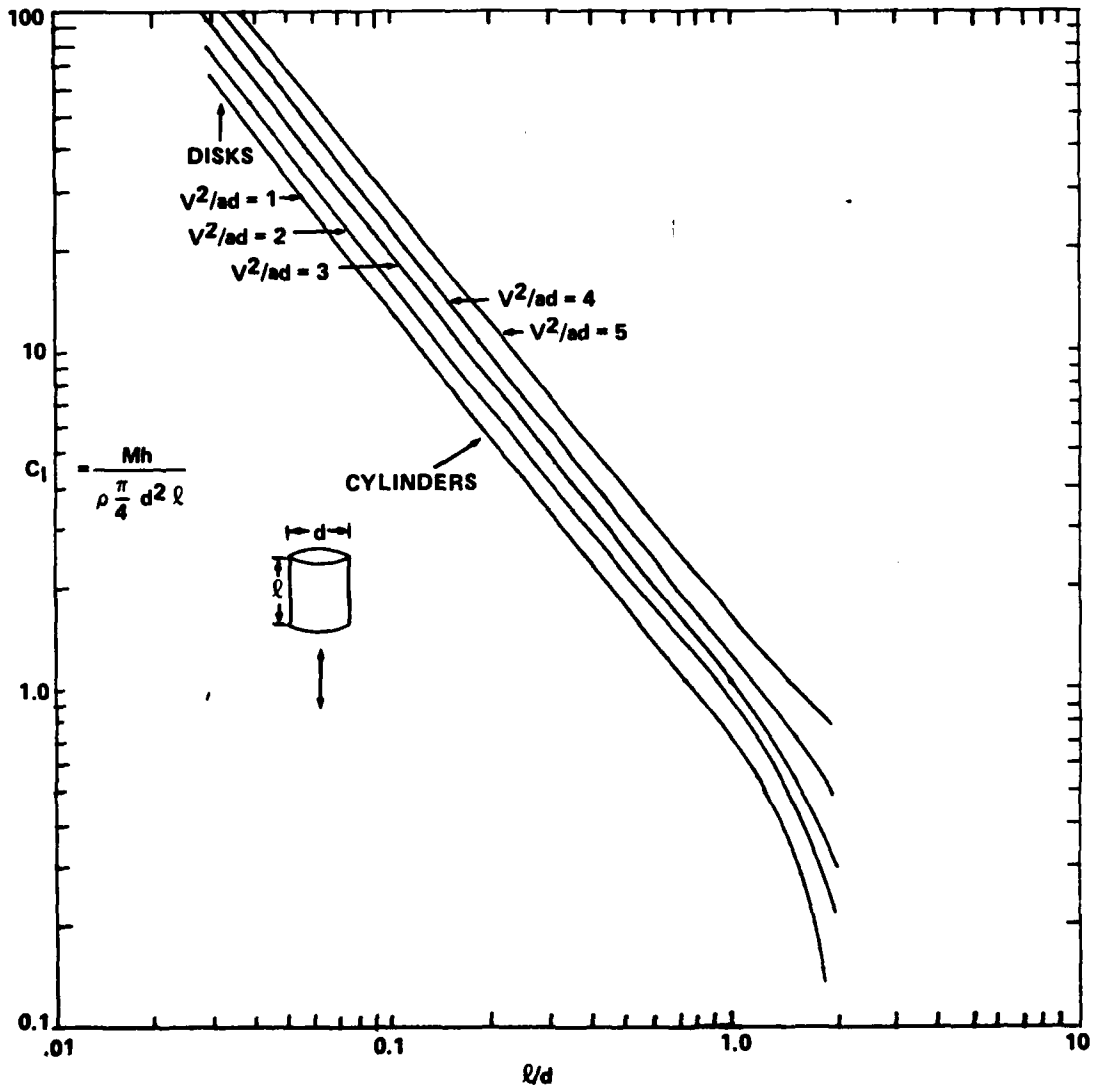


Figure 15. Hydrodynamic Inertia Coefficient Versus Length-To-Diameter Ratio For Oscillating Cylinders.

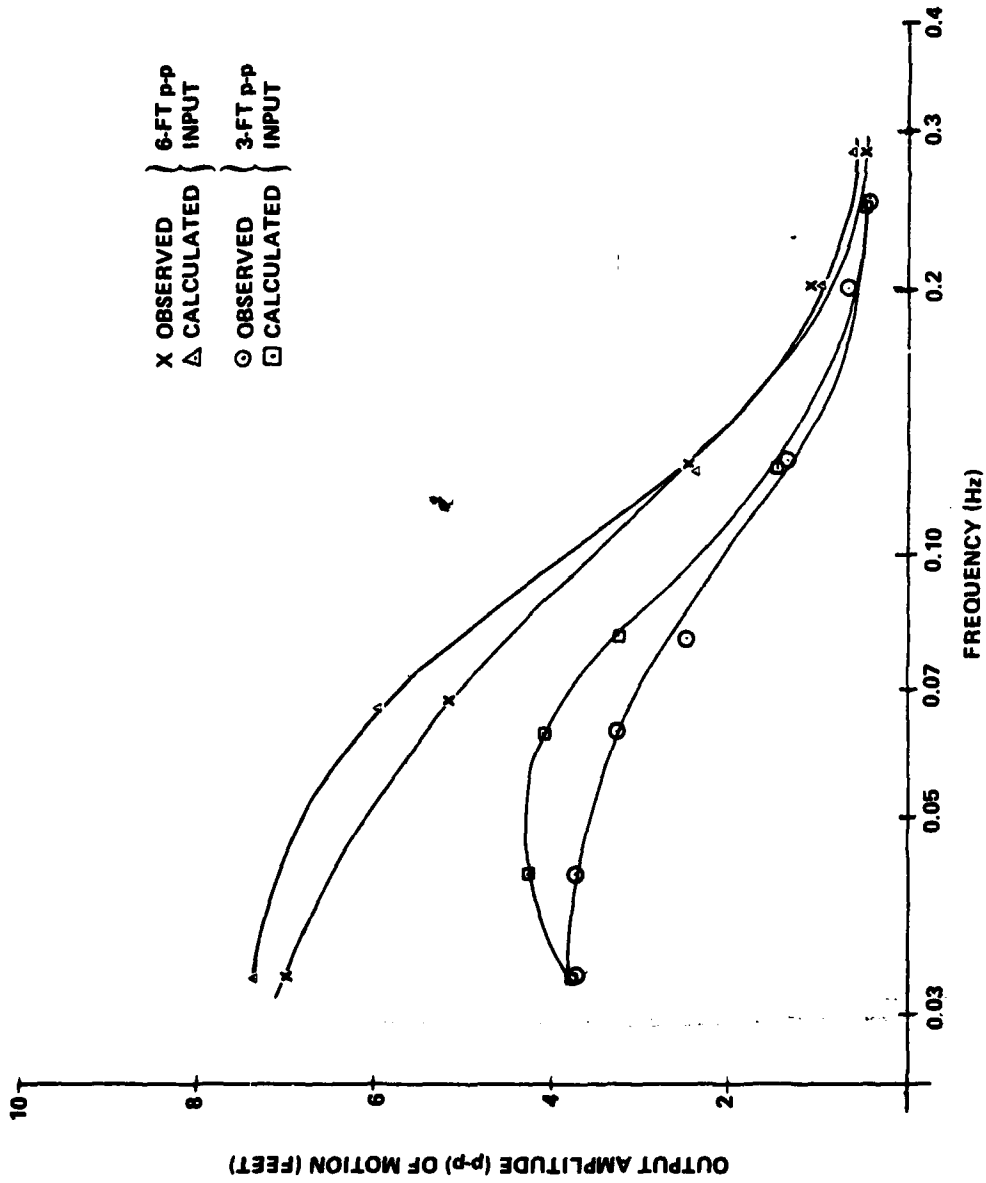


Figure 16. Comparison Of Cylinder ($l/d = 0.75$) Oscillation On 30-Foot Bungee With 3 And 6-Foot p-p Input Amplitudes.

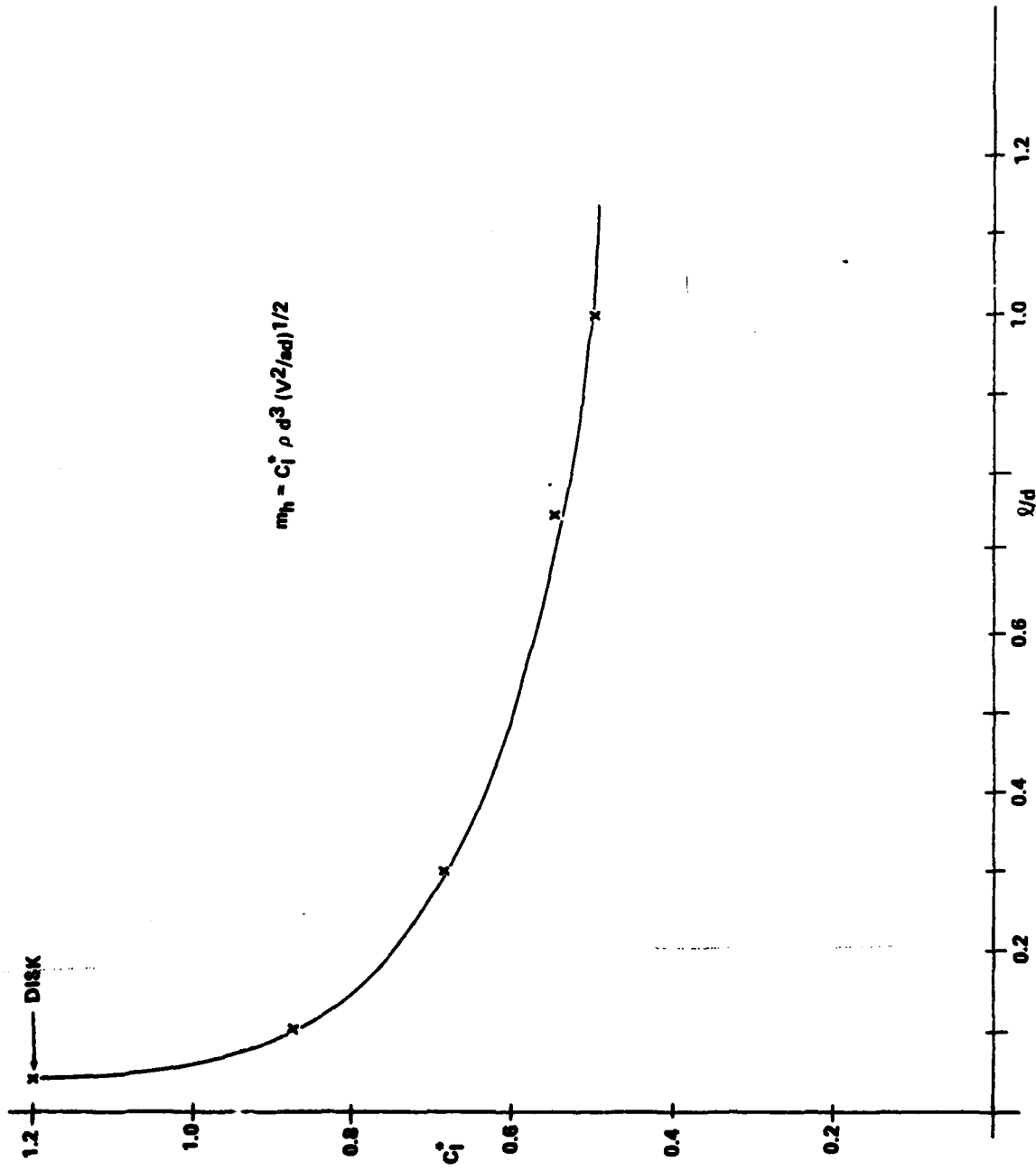


Figure 17. Hydrodynamic Mass Coefficient For Low Aspect Ratio Cylinders For The CABUOY Program (Preliminary).

DISTRIBUTION LIST

REPORT NO. NADC-83112-30

AIRTASK NO. A035-370A/001B/F11-100-300

Work Unit No. ZU701

	No. of Copies
Naval Air Systems Command	6
(2 Copies for AIR-00D4)	
(2 Copies for AIR-370)	
(2 Copies for AIR-549)	
Chief of Naval Operations	2
(2 Copies for OP-3EG)	
Naval Ocean Systems Center	1
(1 Copy for Technical Library)	
Naval Underwater Systems Center, New London	1
(1 Copy for Technical Library)	
Naval Underwater Systems Center, Newport	1
(1 Copy for Technical Library)	
David W. Taylor Naval Ship Research and Development Center	1
(1 Copy for Technical Library)	
Chief of Naval Research	1
(1 Copy for Technical Library)	
Naval Surface Weapons Center, Dahlgren	1
(1 Copy for Technical Library)	
Defense Technical Information Center	12
Naval Air Development Center	3
(3 Copies for Code 8131)	

DATE
FILMED
28